



ACT Project Number:  
**271498**

Project name:  
**ELEGANCY**

Project full title:  
**Enabling a Low-Carbon Economy via Hydrogen and CCS**

**ERA-Net ACT project**

Starting date: 2017-08-31  
Duration: 36 months

## **D2.3.2 Pore and gas sorption properties of Opalinus Clay**

**Date: 2018-07-31**

Organization name of lead participant for this deliverable:  
**Imperial College London**

<b>ACT ELEGANCY, Project No 271498, has received funding from DETEC (CH), FZJ/PtJ (DE), RVO (NL), Gassnova (NO), BEIS (UK), Gassco, Equinor and Total, and is cofunded by the European Commission under the Horizon 2020 programme, ACT Grant Agreement No 691712.</b>		
<b>Dissemination Level</b>		
<b>PU</b>	Public	PU
<b>CO</b>	Confidential , only for members of the consortium (including the Commission Services)	



<b>Deliverable number:</b>	D2.3.2
<b>Deliverable title:</b>	Pore and gas sorption properties of Opalinus Clay
<b>Work package:</b>	WP 2 CO <sub>2</sub> transport, injection and storage
<b>Lead participant:</b>	ICL

<b>Authors</b>		
<b>Name</b>	<b>Organisation</b>	<b>E-mail</b>
Ronny Pini*	ICL	r.pini@imperial.ac.uk
Alireza S Hosseinzadeh Hejazi	ICL	a.hejazi@imperial.ac.uk
Swapna Rabha	ICL	s.rabha@imperial.ac.uk

\*Mark Lead author with asterisk

<b>Keywords</b>
Gas adsorption, Petrophysics, Microporosity

<b>Abstract</b>
<p>Within ELEGANCY, a new decameter-scale experiment will be conducted at the Mont Terri Underground Research Laboratory (URL) in Switzerland aimed at investigating the migration of CO<sub>2</sub>-rich brine through a damaged zone within faults. One of the questions being addressed with this experiment is to what extent the interactions between the CO<sub>2</sub>-rich brine and the rock matrix may limit leakage through a (damaged) caprock. The Opalinus Clay (the main geologic unit at the URL) is characterized by very high clay content and is therefore dominated by nanoscale pores, which provide a large surface area for physical and chemical interactions with the surrounding fluids, including gas adsorption. In this report, we present results from gas adsorption experiments on various dry samples from the URL, including those from the homogeneous shaly facies and the more heterogeneous overburden. The experiments are used to characterize the pore-space of the rock matrix, in terms of metrics, such as the specific surface area and the pore-size distribution. For one sample, CO<sub>2</sub> adsorption experiments have also been conducted over a range of temperatures (10–30°C) and up to 100 kPa. The results indicate that CO<sub>2</sub> adsorption is significant, with uptakes similar to observations on pure clay minerals.</p>



## TABLE OF CONTENTS

---

	Page
1 INTRODUCTION .....	1
2 MATERIALS AND METHODS .....	2
3 PORE SIZE CHARACTERISATION.....	3
4 CO <sub>2</sub> ADSORPTION PROPERTIES.....	5
5 CONCLUDING REMARKS .....	7



## 1 INTRODUCTION

Clay minerals are ubiquitous in the subsurface: they are found in CO<sub>2</sub> sequestration targets (e.g., sandstones) and in the seals above them (Bourg et al. 2015). Clays are also major constituents of unconventional shale plays considered for natural gas recovery (Sone and Zoback 2013). A significant fraction of the porosity in clays and clay-rich systems is occupied by micro- and mesopores that provide a large surface area for physical and chemical interactions with the surrounding fluids, including gas adsorption. The latter results in the creation of a high-density, liquid-like phase on the pore walls, which has important implications on the storage of gas (Busch et al. 2016) and on its transport through the microporous matrix of the rock (Allan and Mavko 2013). While these natural materials are weakly sorbing when compared to known industrial microporous adsorbents, such as zeolites or carbons, the large bulk density of rocks (~2.5 g/cm<sup>3</sup>) and the large spatial footprint of geologic formations suggest that the actual contribution of gas adsorption in these systems may still be significant. From a practical perspective, and with relevance to CO<sub>2</sub> storage, gas adsorption on clay-rich rocks may contribute to increased storage security by limiting gas diffusion through the seals above the host reservoir.

Experiments and pilot-scale tests are needed to understand the mechanisms controlling fluid migration through seals above potential CO<sub>2</sub> sequestration sites. This is key towards quantifying the effective mobility of CO<sub>2</sub> in caprocks and in the overburden. Within ELEGANCY, this challenge is addressed by executing a decameter-scale experiment at the Mont Terri URL in Switzerland. The experiment will enable direct observation of fluid migration along a fault and of its interaction with the surrounding environment. Recent experiments at the Mont Terri URL have indicated that sub-millimetre slip movements (0.01 – 0.1 mm) can create permeable paths across a fault-zone without producing significant seismic activity (Guglielmi et al. 2017). How such peculiar permeability behavior may affect the migration of CO<sub>2</sub> remains to be answered. In particular, one of the questions being addressed with the experiment is to what extent the interactions between the CO<sub>2</sub>-rich brine and the rock matrix may limit leakage through a (damaged) caprock. Of particular interest to this study is the adsorption behaviour of CO<sub>2</sub>, because the Opalinus Clay (the main geologic unit at the URL) is characterized by very high clay content. For the shaly facies and the carbonate-rich sandy facies, the clay content may reach values as high as 80wt% and 45wt%, respectively (Bossart et al. 2017), thus providing sites for adsorption reactions to occur.

A core-analysis campaign is being designed to provide detailed petrophysical characterization of rock samples collected at the Mont Terri URL, both from the damaged fault rocks and from the undisturbed rocks. In this report, we will present results from gas adsorption experiments on various dry samples from the Mont Terri URL, including those from the homogeneous shaly facies and the more heterogeneous overburden.

## 2 MATERIALS AND METHODS

The samples used in this study are listed in Table 1 and have been cored at the Mt Terri Underground Research Laboratory from boreholes BPE-1, BPE-2 and BPE-3 (see Report D2.3.1 for more information regarding the locations of the boreholes). The samples were selected, so as to represent both shaly- and carbonate-rich facies of the Opalinus Clay (BPE-1), in addition to the heterogeneous overburden (Passwang Formation, BPE-2 and BPE-3). In this report, a selection of measurements carried out on samples from each borehole will be presented (labelled with a “star” on Table 1). A photograph of the four (as-received) samples used in this study is shown in Figure 1. The two samples from BPE-1 are from the shaly facies; the sample cored at 7.3 m is fairly homogeneous, while the one cored at 31.1 m contains characteristic thin sand lenses. The other two samples (BPE-2 64m and BPE-3 21.0m) are lime-rich and are both visually more heterogeneous.

*Table 1 - Samples obtained from the Mt Terri Underground Research Laboratory and their properties. The samples labelled with \* have been used in this characterization study.*

Well	Interval / m	Core length / cm	Formation	Comments
BPE-1				
1*	7.03 – 7.65	62	OPA	Homogeneous shaly facies
2	30.50 – 30.60	45	OPA	Carbonate-rich facies with bioturbation lenses
3*	31.10 – 31.55	20	OPA	Shaly facies with sand lenses
BPE-2				
4*	64.65 – 65.05	40	PW	Oolitic marl with cracks
BPE-3				
5	19.20 – 19.75	55	PW	Carbonatic limestone with bioturbation
6*	19.25 – 20.25	30	PW	Carbonatic limestone with iron ooids

A Quantachrome Autosorb iQ-MP sorption analyser was used to perform adsorption studies on the four samples with N<sub>2</sub> at 77K and with CO<sub>2</sub> at various temperatures (10–30°C) in the pressure range  $p < 100$  kPa. For these experiments, a small amount of sample (150 – 200 mg) was obtained from the main core and gently ground to a particle size of < 90 microns. Prior to each experiment, the samples were degassed at 120°C for about 16 hours. The same regeneration procedure was applied in a previous study on the source clay Na-Montmorillonite (Hwang et al. 2019) and was established based on observations from both thermo-gravimetric analysis (TGA) and differential thermal gravimetry (DTG) measurements (Kuila and Prasad 2013).



*Figure 1- Photograph of the core samples used in this study.*

### 3 PORE SIZE CHARACTERISATION

The microscopic structural properties of the four samples were determined via low-pressure physisorption analysis, which was conducted using  $N_2$  at 77 K in the pressure range  $p/p^0 = 1 \times 10^{-6} - 0.99$ , where  $p^0 = 0.1$  MPa is the reference atmospheric pressure. The results from these experiments are shown in Figure 2, where it can be seen that the amount adsorbed increases in the order BPE-3 21.0 < BPE-1-31.3 < BPE-1 7.3 < BPE-2 64.7. Experiments were carried out in both adsorption (empty symbols) and desorption modes (filled symbols). All isotherms are of type II with a hysteresis loop of type H3 according to the classification by Thommes et al. 2015. The adsorbed amount increases as  $p/p^0$  reaches unity without reaching a plateau, indicating that all samples contain both meso- and macro-pores. Moreover, at very low pressures ( $p/p^0 < 0.1$ ), a steep increase in the adsorbed amount is observed, suggesting that the four sample also have a noticeable level of micropore filling. The latter is particularly evident for both the homogeneous shaly sample (BPE-1 7.3) and for the oolitic marl (BPE-2 64.7).

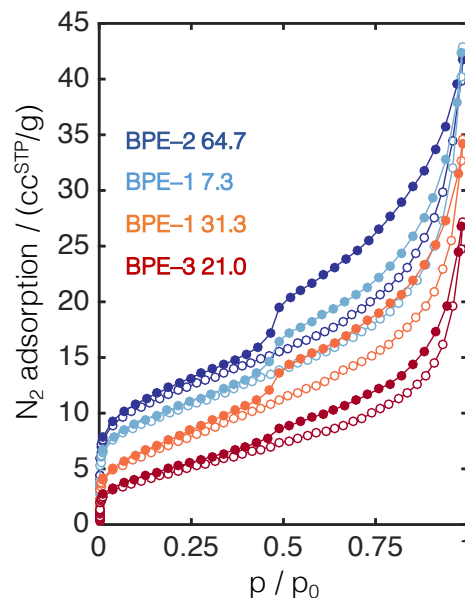


Figure 2 -  $N_2$  physisorption isotherms measured at 77 K on four different samples from the Mt Terri Underground Laboratory (Table 1). The empty and filled symbols refer to measurements taken in adsorption and desorption mode, respectively.

The specific surface area (SSA) of each sample was estimated using the linear form of the BET equation (Brunauer et al. 1938), which is used to derive the value of the monolayer capacity formed by evenly distributed adsorbed molecules with a given value of the molecular area ( $0.162 \text{ nm}^2$  for  $N_2$ ). The estimated SSA for the four values are reported in Table 2 and follow the same order observed in the amount adsorbed (Figure 2), namely  $18.1 \text{ m}^2/\text{g}$  (BPE-3 21.0) <  $27.4 \text{ m}^2/\text{g}$  (BPE-1-31.3) <  $35.9 \text{ m}^2/\text{g}$  (BPE-1 7.3) <  $42.1 \text{ m}^2/\text{g}$  (BPE-2 64.7). As a means of comparison, the reported SSA of pure montmorillonite clay takes a value of  $\sim 32 \text{ m}^2/\text{g}$  (Hwang et al. 2019).

The pore volume and the pore-size distribution of micro- (width smaller than 2 nm), meso- (width smaller than 50 nm) and macro-pores (widths larger than 50 nm) were evaluated by the application of the DFT kernel provided with the instrument's software. The obtained pore volumes of each

ACT ELEGANCY, Project No 271498, has received funding from DETEC (CH), FZJ/PTJ (DE), RVO (NL), Gassnova (NO), BEIS (UK) and Gassco AS, and is cofunded by the European Commission under the Horizon 2020 programme, ACT Grant Agreement No 691712.

sample are summarized in Table 2, together with the model-predicted values of the SSA. It can be seen that a fair agreement is observed between estimates from the conventional BET method and DFT predictions with deviations in the order of 10–20%. The estimated total pore volumes increase in the same order as the SSA and range between 0.032 mL/g (BPE-3 21.0) and 0.054 mL/g (BPE-2 64.7). These values are somewhat smaller than previous observations on the pure Na-Montmorillonite clay (0.09 mL/g).

Table 2 – Specific surface areas (SSA) and pore volumes ( $V_p$ ) of four samples from the Mt Terri Underground Research Laboratory. The subscript DFT refer to estimates from the DFT kernel.

Sample	Interval / m	SSA <sub>BET</sub> [m <sup>2</sup> /g]	SSA <sub>DFT</sub> [m <sup>2</sup> /g]	V <sub>p,DFT</sub> [cc/g]
1	7.03 – 7.65	35.9	33.1	0.052
3	31.10 – 31.55	27.4	22.7	0.043
4	64.65 – 65.05	42.1	38.3	0.054
6	19.25 – 20.25	18.1	14.6	0.032

The corresponding pore size distributions of the four porous samples are plotted in Figure 3 against the pore diameter  $d_p$  in terms of both differential,  $dV(r)/dr$ , and cumulative pore volumes,  $V(r)$ . Note that for the sake of clearer visualization only the range  $0 < d_p < 20$  nm is shown in the figure. Interestingly, it can be seen that the majority of the pore space (~70% of the total) is contained in pores smaller than 20 nm. Moreover, for samples BPE-1 7.3 (homogeneous shaly facies) and BPE-2 64.7 (oolitic marl), 20% of the total porosity is included in the micropores ( $d_p < 2$  nm), as opposed to the other two samples, where the majority of the pore space is in the mesopores ( $d_p > 2$  nm).

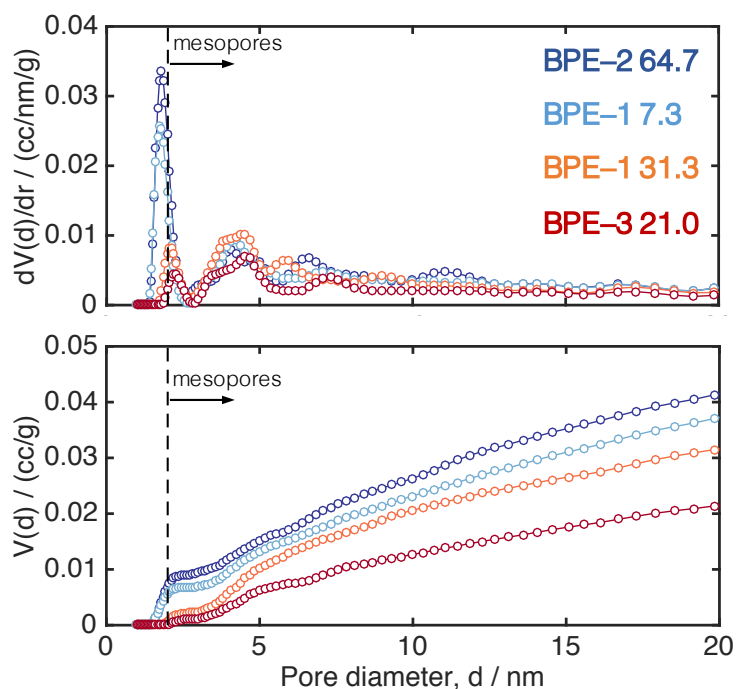


Figure 3 – Differential (top) and cumulative (bottom) pore size distribution for the four samples from the Mt Terri Underground Laboratory.

## 4 CO<sub>2</sub> ADSORPTION PROPERTIES

Gas adsorption experiments with CO<sub>2</sub> were carried out on sample BPE–1 7.3 (homogeneous shaly), this being the sample with a relatively large surface area. The experiments were carried out at three different temperatures (10, 20 and 30°C) and the results are shown in Figure 4. It can be seen that adsorption increases with pressure and decreases with increasing temperature. At a pressure of 100 kPa, the amount of CO<sub>2</sub> adsorbed is about 200 μmol/g (10°C), 150 μmol/g (20°C) and 90 μmol/g (30°C). Again, these results are comparable to observations on the source-clay Na-Montmorillonite for which the amount CO<sub>2</sub> adsorbed was ~100 μmol/g at 100 kPa and 25°C (Hwang et al. 2019). In Figure 4, the symbols are experimental results, while the lines have been obtained by fitting the Langmuir adsorption model to the experimental data:

$$V = \frac{V^{\infty} bp}{1 + bp}$$

where  $V^{\infty}$  refer to the monolayer capacity and  $b$  is the Langmuir constant. The values of the fitted parameters are reported in Table 3. It can be seen that the isotherms can be described by the Langmuir model by using a monolayer capacity that is temperature-independent ( $V^{\infty} = 35.2$  cc<sup>STP</sup>/g). We note that if CO<sub>2</sub> were to fill by adsorption the entire pore volume of the sample, the latter would take a value of 0.0574 – 0.0674 cc/g (upon assuming a density of the adsorbed phase of 23–27 mol/L, as reported in Pini 2014), which is slightly larger than the value estimated from the DFT kernel (Table 2). Accordingly, one would expect that at 30°C and 100 kPa, about 50% of the micropores would be filled with adsorbed CO<sub>2</sub> ( $V = 0.0033$  – 0.0039 cc/g).

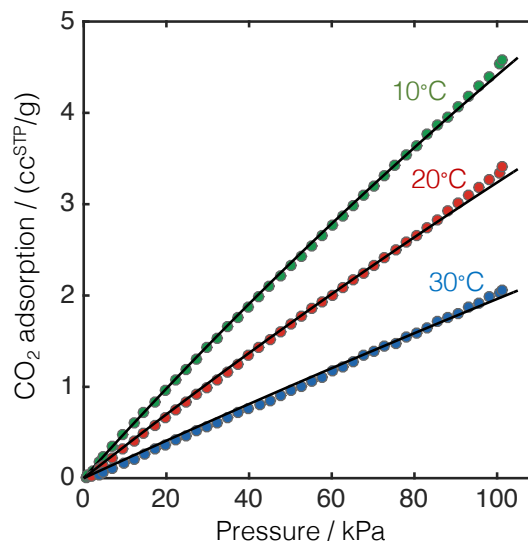


Figure 4 – CO<sub>2</sub> adsorption isotherms at 10, 20 and 30°C measured on sample BPE–1 7.3 (homogeneous shaly) from the Mt Terri Underground Laboratory. Symbols are experimental results, while the solid lines refer to fits using the Langmuir adsorption model.

In Table 3 are reported also the values of the Henry's constants,  $H = V^{\infty} b$ , for sample BPE–1 7.3 at the three measured temperatures. The Henry's constant is commonly regarded as one of the

ACT ELEGANCY, Project No 271498, has received funding from DETEC (CH), FZJ/PTJ (DE), RVO (NL), Gassnova (NO), BEIS (UK) and Gassco AS, and is cofunded by the European Commission under the Horizon 2020 programme, ACT Grant Agreement No 691712.

fundamental parameters that describes an adsorbate-adsorbent pair. Its accurate determination is required in the calculation of other relevant thermodynamic properties, such as the enthalpy of adsorption. It can be seen from the table that the values of the Henry's constants decrease with increasing temperature, as expected based on thermodynamic considerations. The obtained values are plotted in Figure 5, alongside results for the source-clay Na-Montmorillonite (Hwang et al. 2019). It can be seen that when plotted as a function of the inverse of temperature, the obtained Henry's constants follow a correlation of the following form:

$$H = H_0 e^{(-\Delta h_0/RT)}$$

where  $\Delta h_0$  is the zero-coverage enthalpy of adsorption. Accordingly,  $\Delta h_0$  is the negative value of the slope of the linear fit obtained from plotting  $\ln(H)$  against  $1/T$  multiplied by the ideal gas constant,  $R$ . We note that the value of  $\Delta h_0$  is negative due to the exothermic nature of adsorption, and it is common to refer to its absolute value as the isosteric heat. The obtained values of the isosteric heat for  $\text{CO}_2$  adsorption on BPE-1 7.3 have been estimated to be  $-31.6$  kJ/mol. The common perception for physisorption is that  $\Delta h_0/\Delta h_{vap} < 1.5 - 2$  (Ruthven 1991), where  $\Delta h_{vap}$  is the latent heat of vapourisation. Because for  $\text{CO}_2$  at 273.15 K,  $\Delta h_{vap} = -10.3$  kJ/mol, we contend that the obtained estimates on BPE-1 may be an overestimate. Further work is required to understand the reasons for this and will include new experiments over a wider range of temperatures.

Table 3 – Langmuir constants and Henry's constants for sample BPE-1 7.3

T [°C]	$V_\infty$ [cc <sup>STP</sup> /g]	b [kPa <sup>-1</sup> ]	H [cc <sup>STP</sup> g <sup>-1</sup> kPa <sup>-1</sup> ]
10	35.2	$1.43 \times 10^{-3}$	0.0504
20		$1.01 \times 10^{-3}$	0.0357
30		$0.59 \times 10^{-4}$	0.0208

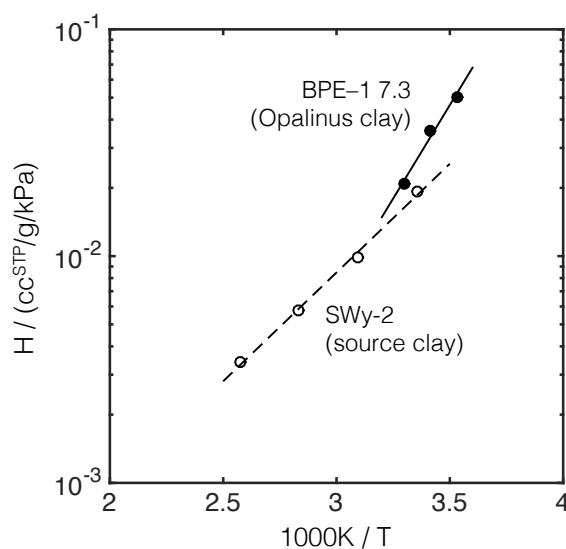


Figure 5 – Henry's constants plotted as a function of the temperature for  $\text{CO}_2$  measurements on BPE-1 7.3 (this study, filled symbols) and the source-clay Na-Montmorillonite (SWy-2, empty symbols, Hwang et al. 2019).

## 5 CONCLUDING REMARKS

In this report, results from gas adsorption studies on four samples from the Mont Terri URL have been presented. The results from the experiments with N<sub>2</sub> have been used to provide estimates of the pore space properties of both the Opalinus Clay and the Passwang formation. It is observed that the pore space of the rocks is largely mesoporous; for the homogeneous shaly facies and the oolitic marl, the pore space includes also a significant fraction of microporosity (20vol%). CO<sub>2</sub> adsorption experiments have been carried out on the sample from the homogeneous shaly facies. The data suggest that the uptake is significant and similar to observations on source-clays. To confirm these findings, additional observations are required, including adsorption experiments in the presence of water and at higher pressures, so as to better represent the conditions found at depth.

## APPENDIX

### A REFERENCES

- A.M. Allan, G. Mavko (2013) The effect of adsorption and Knudsen diffusion on the steady-state permeability of microporous rocks. *Geophysics*, 78, D75–D83
- Bossart P, F Bernier, J Birkholzer, C Bruggeman, P Connolly et al. (2017) Mont Terri rock laboratory, 20 years of research: introduction, site characteristics and overview of experiments. *Swiss J Geosci*, 110, 3–22.
- I.C. Bourg, L.E. Beckingham, D.J. DePaolo (2015) The Nanoscale Basis of CO<sub>2</sub> Trapping for Geologic Storage, *Environ Sci Technol* 49, 10265–10284
- S. Brunauer, P.H. Emmett, E. Teller (1938) Adsorption of Gases in Multimolecular Layers. *J Am Chem Soc*, 60, 309–319.
- A. Busch, P. Bertier, Y. Gensterblum, G. Rother, C.J. Spiers, M. Zhang, H.M. Wentinck (2016) On sorption and swelling of CO<sub>2</sub> in clays, *Geomechanics and Geophysics for Geo-energy and Geo-resources*, 2, 111–130
- Guglielmi Y, J Birkholzer, J Rutqvist, P Jeanne, C Nussbaum (2017) Can Fault Leakage Occur Before or Without Reactivation? Results from an In Situ Fault Reactivation Experiment at Mont Terri. *Energy Procedia*, 114, 3167–74.
- J. Hwang, L. Joss, R. Pini (2019) Measuring and modelling supercritical adsorption of CO<sub>2</sub> and CH<sub>4</sub> on montmorillonite source clay. *Micropor Mesopor Mat*, 273, 107–121.
- U. Kuila, M. Prasad (2013) Specific surface area and pore-size distribution in clays and shales. *Geophys Prospect*, 61, 341–362.
- R. Pini (2014) Interpretation of net and excess adsorption isotherms in microporous adsorbents. *Microporous and Mesoporous Materials*, 187, 40–52.
- D. M. Ruthven (1991) Adsorption. *Kirk–Othmer Encyclopedia of Chemical Technology*.
- H. Sone, M.D. Zoback (2013) Mechanical properties of shale-gas reservoir rocks — Part 1: Static and dynamic elastic properties and anisotropy. *Geophysics* 78, D381–D392.
- M. Thommes, K. Kaneko, A.V. Neimark, J.P. Olivier, F. Rodriguez-Reinoso, et al. (2015) Physisorption of gases, with special reference to the evaluation of surface area and pore size distribution (IUPAC Technical Report). *Pure Appl Chem*, 87, 1051–1069.